Supplementary Information

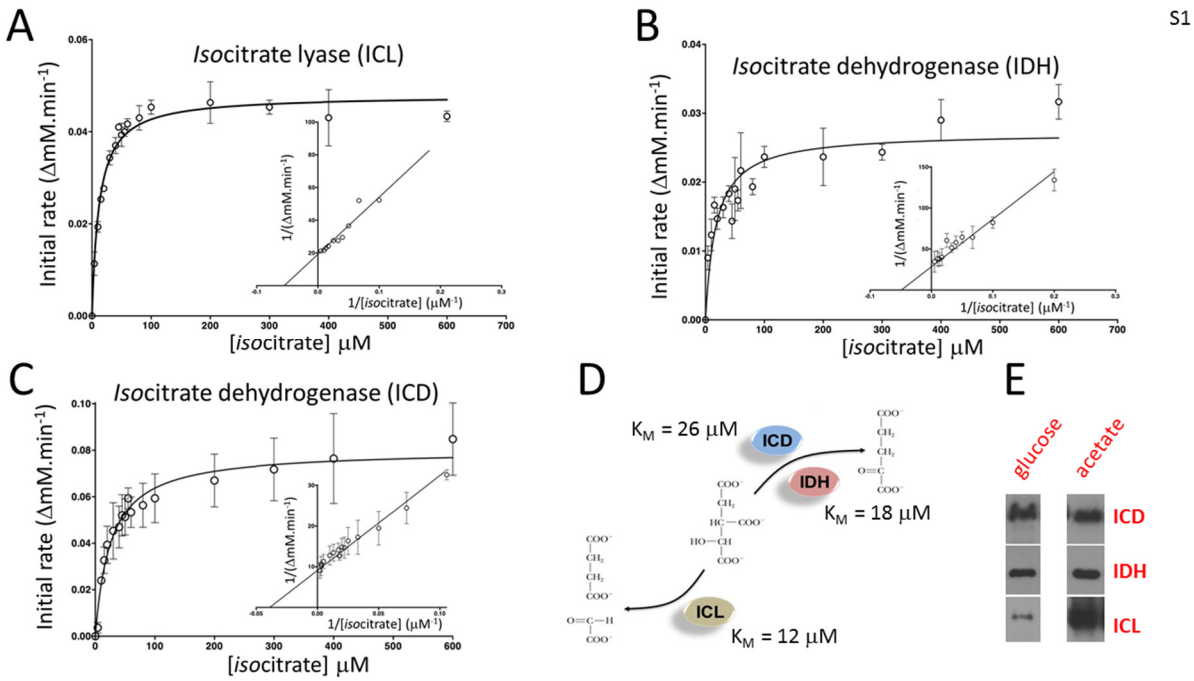

Figure S1. Enzyme kinetics (*iso*citrate dependency) of *P. aeruginosa* ICL **(A)**, IDH **(B)** and ICD **(C)**. The main body of each panel shows the direct plot and the insert shows the corresponding Lineweaver-Burk transformation. Extracted kinetic constants are shown in **Table I**. Each assay was performed in triplicate. Error bars correspond to ± 1 standard deviation. **(D)** Schematic showing the calculated K_M (*iso*citrate) of each enzyme and the reaction catalysed. **(E)** Semi-quantitative Western blot showing that ICD and IDH are expressed at similar levels during growth on glucose or acetate, and that ICL is expressed during growth on glucose but that the level of enzyme expression increases during growth on acetate.

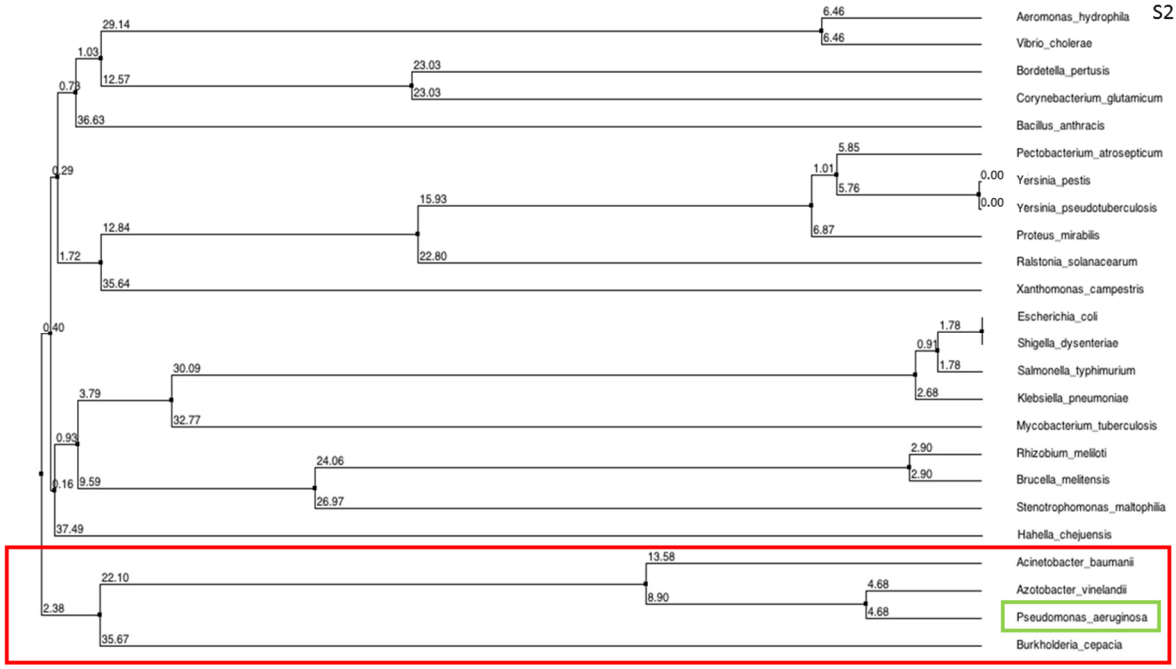

Figure S2. Phylogenetic tree of ICL from a subset of pathogens. Note how the *P. aeruginosa* ICL forms a distinct cluster (boxed in red) with ICL from *Acinetobacter baumanii*, *Azotobacter vinelandii* and *Burkholderia cepacia*. The tree was generated after alignment of all amino acid sequences using ClustalOmega and neighbour joining was calculated from the percentage sequence identity in JalView.

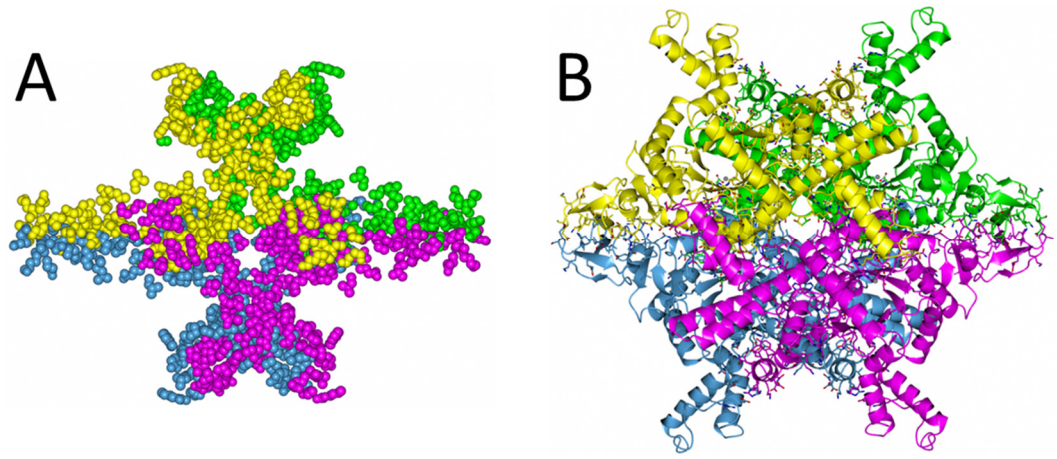

Figure S3. The *P. aeruginosa* ICL tetramer is held together by numerous inter-subunit bonds contributed by each protomer. **(A)** Space-filling view of the residues involved in tetramerisation of *P. aeruginosa* ICL. **(B)** The same residues represented as sticks supported by each protomer of the tetramer. The data shown are based on a COCOMAPS estimation, and the total excluded surface area is 12,352 $Å^2$.

GFC/MALS and AUC data for *P. aeruginosa* ICL

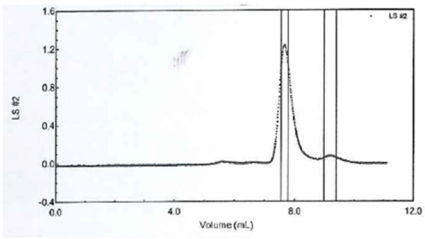

RESULTS		PEAK #1	PEAK #2
Volume (mL)	:	7.550 - 7.775	8.992 - 9.400
Slices	:	28	50
A2 (mol mL/g²)	:	0.000e+00	0.000e+00
Fit degree	:	1	1
Injected Mass (g)	:	4.0000e-05	4.0000e-05
Calc. Mass (g)	:	2.2118e-05	-4.8533e-07
dn/dc (mL/g)	:	0.185	0.185
Polydispersity(Mw/Mn)	:	1.001±0.009 (0.9%)	1.077±0.265 (25%)
Polydispersity(Mz/Mn)	:	1.002±0.015 (1.5%)	1.230±0.622 (51%)
Molar Mass Moments (g/mol)			
Mn	:	2.318e+05 (0.6%)	1.845e+07 (15%)
Mw	:	2.321e+05 (0.6%)	1.988e+07 (18%)
Mz	:	2.323e+05 (1.4%)	2.270e+07 (48%)

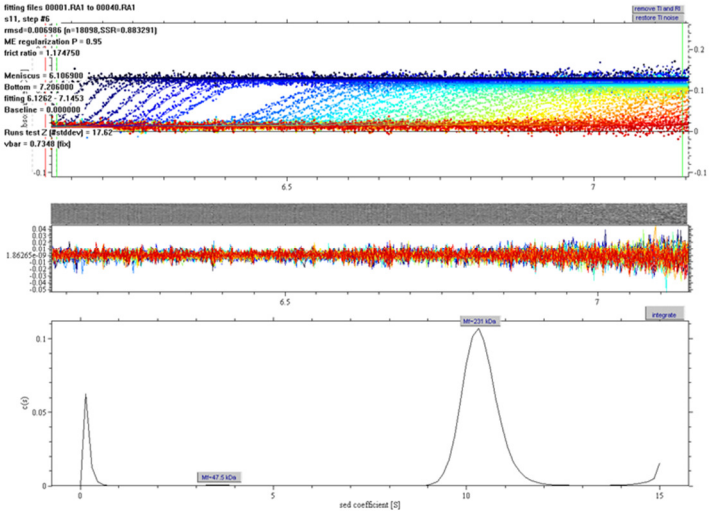

Gel Filtration/MALS

Analytical Ultracentrifugation

Figure S4. Solution structure of ICL determined by gel filtration chromatography coupled with multi-angle light scattering (GFC-MALS) and analytical ultracentrifugation (AUC). The overall molecular mass of ICL inferred from GFC-MALS analysis was 232 kDa. AUC analysis yielded a very similar estimated molecular mass of 231 kDa. Given that the calculated molecular mass of one ICL polypeptide is 59 kDa, *iso*citrate lyase is likely to be a tetramer (M_w = 236 kDa) in solution.

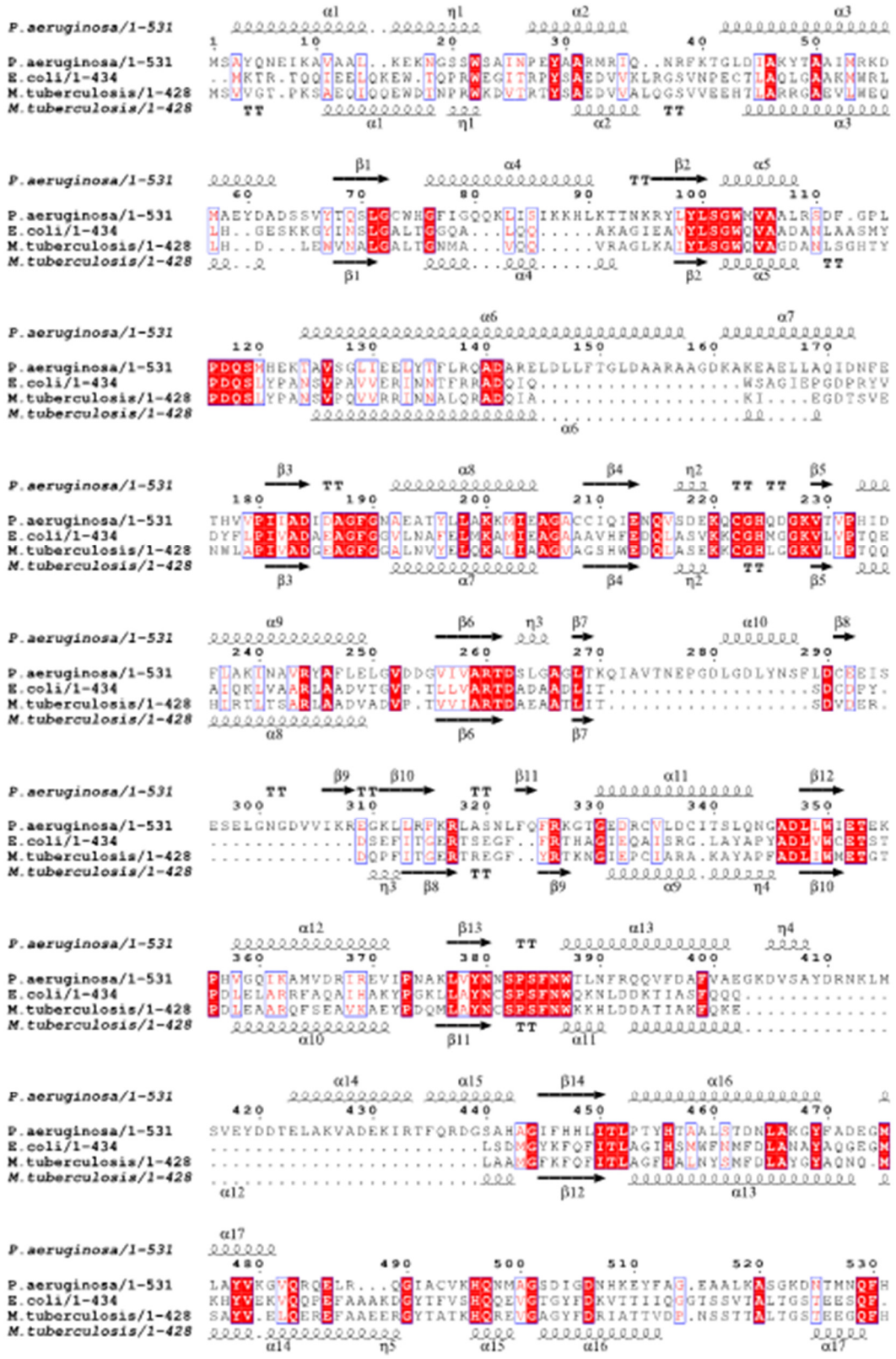

Figure S5. ESPript alignment and secondary structure analysis of *iso*citrate lyase from *P. aeruginosa*. The amino acid sequences of ICL from *P. aeruginosa*, *E. coli* and *M. tuberculosis* are shown, along with the corresponding secondary structure assignments (*P. aeruginosa* on the top row and *M. tuberculosis* (PDB 1F8I) on the bottom row).

GFC/MALS data for *P. aeruginosa* IDH

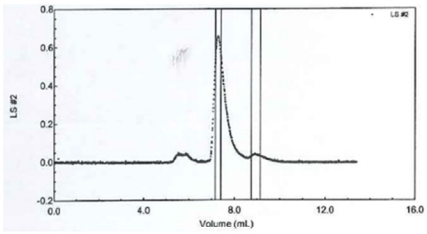

RESULTS		PEAK #1	PEAK #2
Volume (mL)	:	7.167 - 7.400	8.742 - 9.133
Slices	:	29	48
A2 (mol mL/g²)	:	0.000e+00	0.000e+00
Fit degree	:	1	1
Injected Mass (g)	:	4.0000e-05	4.0000e-05
Calc. Mass (g)	:	1.2148e-05	2.3181e-06
dn/dc (mL/g)	:	0.185	0.185
Polydispersity(Mw/Mn)	:	1.000±0.015 (1.5%)	1.027±0.272 (26%)
Polydispersity(Mz/Mn)	:	1.000±0.025 (2.5%)	1.061±0.523 (49%)
Molar Mass Moments (g/mol)			
Mn	:	2.355e+05 (1.0%)	1.373e+05 (17%)
Mw	:	2.356e+05 (1.0%)	1.409e+05 (19%)
Mz	:	2.356e+05 (2.3%)	1.456e+05 (45%)

Gel Filtration/MALS

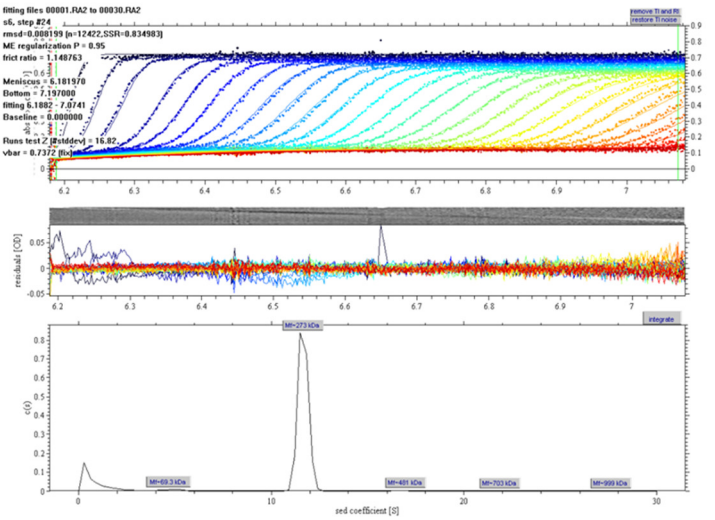

Analytical Ultracentrifugation

Figure S6. Solution structure of IDH determined by gel filtration chromatography coupled with multi-angle light scattering (GFC-MALS) and analytical ultracentrifugation (AUC). The overall molecular mass of IDH inferred from GFC-MALS analysis was 236 kDa. AUC analysis yielded a higher estimated molecular mass of 273 kDa. Given that the calculated molecular mass of one IDH polypeptide is 82 kDa, these data suggest that IDH could be a trimer or elongated dimer in solution. However, we also note that the protein has a rather low frictional coefficient (f = 1.15), consistent with it adopting a compact, globular configuration.

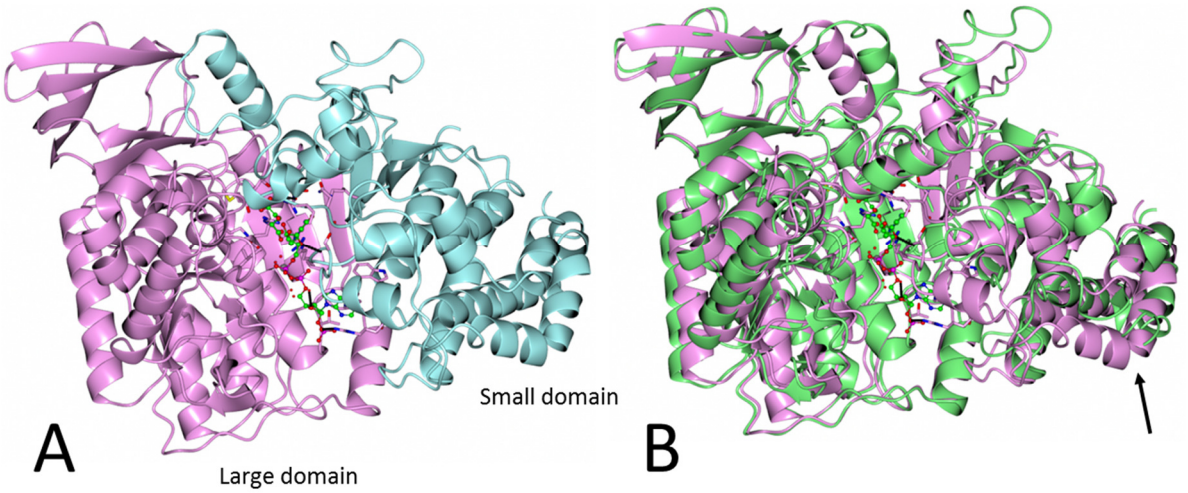

Figure S7. IDH domains and conformational differences in the presence of bound reactions products. The figure shows a cartoon representation of *P. aeruginosa* IDH. **(A)** IDH is comprised of two domains; a large one (mauve) spanning Leu139 - Leu571, and a small one (teal) spanning Ser5 - Val138 and Met572 - Ala741. **(B)** Superposition of IDH chain A (mauve) and chain B (light green). The conformational differences between each polypeptide chain affect most parts of the molecule, although they are particularly obvious in the small domain in the region marked by the arrow.

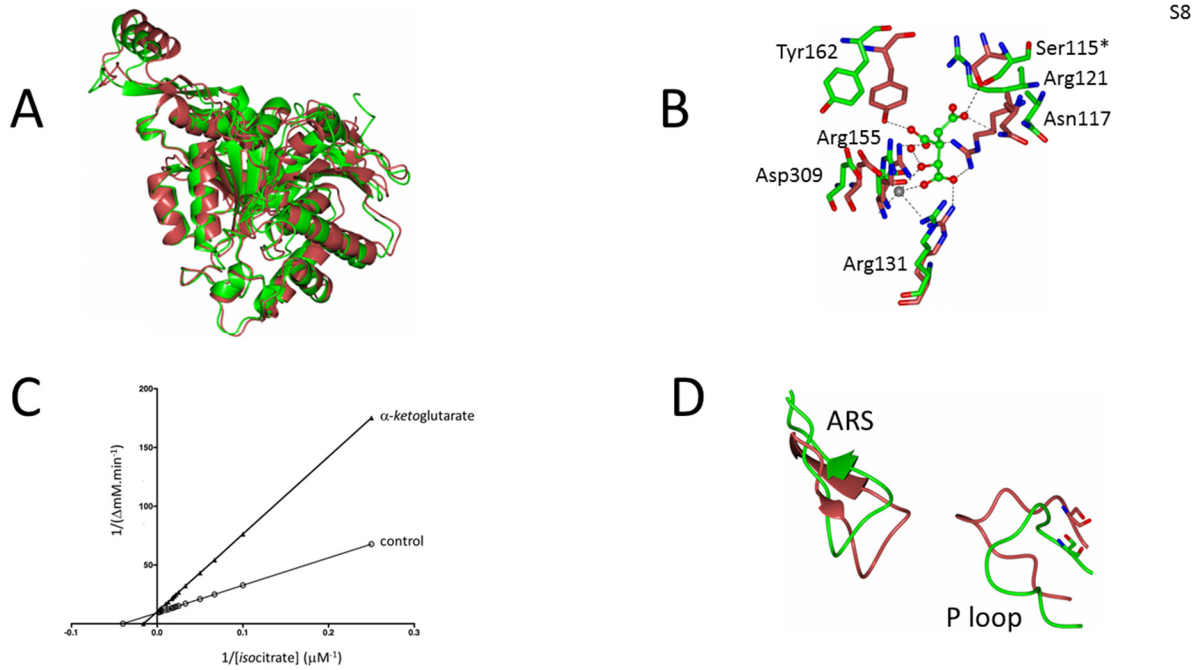

Figure S8. Structure and kinetics of *P. aeruginosa iso*citrate dehydrogenase (ICD). **(A)** The overall structure of *P. aeruginosa* ICD is very similar to that of *E. coli* ICD. The panel shows a superposition of the *P. aeruginosa* structure (green, PDB 5M2E) and the *E. coli* ICD structure (red, PDB 4AJA). The only significant structural difference between the proteins is that in the projection forming the clasp-like dimerization determinant, the *P. aeruginosa* structure forms a large β-strand (encompassing residues Cys196 to Ser204) that is absent in the *E. coli* protein. Overall, the secondary structures superimpose with an RSMD of 1.94 Å. **(B)** The known catalytic residues in *E. coli* ICD_{EC} (red, PDB 4AJA) are conserved in *P. aeruginosa* ICD (green, PDB 5M2E). The ball-and-stick molecule of *iso*citrate and the Mg^{2+} (gray) shown in this panel are modelled from the *E. coli* ICD structure, since these are not present in the *P. aeruginosa* ICD structure. The absence of substrate in the *P. aeruginosa* apo structure likely explains why not all of the side chains point inwards to coordinate the *iso*citrate. **(C)** ICD is feedback inhibited by α-*keto*glutarate. A Lineweaver-Burk analysis indicates that the inhibition is competitive. **(D)** The AceK recognition motifs are conserved in the *P. aeruginosa* ICD structure. The configuration of the ARS and P-loop are similar in ICD_{PA} (green) and ICD_{EC} (red).

GFC/MALS and AUC data for *P. aeruginosa* ICD

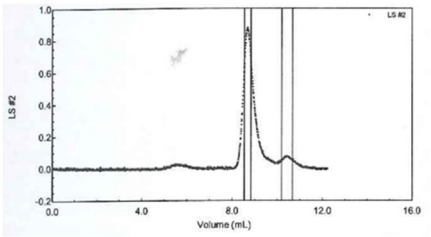

RESULTS		PEAK #1	PEAK #2
Volume (mL)	:	8.550 - 8.833	10.192 - 10.667
Slices	:	35	58
A2 (mol mL/g²)	:	0.000e+00	0.000e+00
Fit degree	:	1	1
Injected Mass (g)	:	4.0000e-05	4.0000e-05
Calc. Mass (g)	:	4.8947e-05	5.6701e-06
dn/dc (mL/g)	:	0.185	0.185
Polydispersity(Mw/Mn)	:	1.001±0.010 (1.0%)	1.024±0.126 (12%)
Polydispersity(Mz/Mn)	:	1.002±0.017 (1.7%)	1.049±0.223 (21%)
Molar Mass Moments (g/mol)			
Mn	:	9.070e+04 (0.7%)	1.129e+05 (8%)
Mw	:	9.079e+04 (0.7%)	1.156e+05 (8%)
Mz	:	9.087e+04 (1.6%)	1.184e+05 (19%)

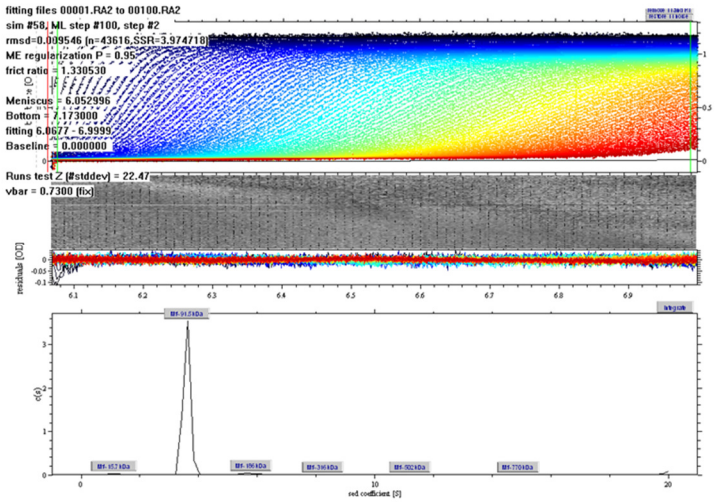

Gel Filtration/MALS Analytical Ultracentrifugation

Figure S9. Solution structure of ICD determined by gel filtration chromatography coupled with multi-angle light scattering (GFC-MALS) and analytical ultracentrifugation (AUC). The overall molecular mass of ICD inferred from GFC-MALS analysis was 90 kDa. AUC analysis yielded a very similar estimated molecular mass of 91.5 kDa. Given that the calculated molecular mass of one ICD polypeptide is 45 kDa, the ICD *iso*citrate dehydrogenase is likely to be a dimer (M_w = 90 kDa) in solution.

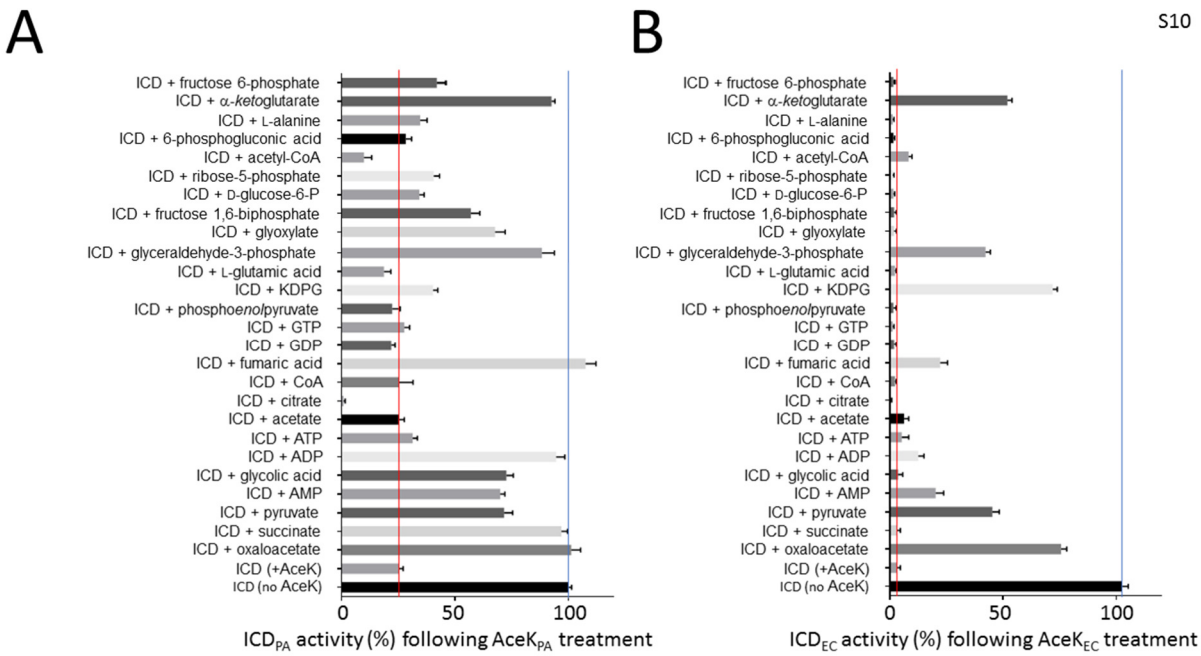

Figure S10. Impact of small molecule regulators of AceK kinase/phosphatase activity. **(A)** ICD_{PA} was first inactivated by incubation for 60 min with $AceK_{PA}$ and ATP. Following this, the indicated small molecule regulators were added (5 mM final concentration in all cases) and the reaction was allowed to continue for a further 30 min. The *iso*citrate dehydrogenase activity of each sample was then measured. Note how ICD retains about 25% of its activity even after extensive treatment with AceK, unless acetyl-CoA or citrate are present (see main text for details). The blue line represents the activity of ICD that has not been treated with AceK and the red line indicates the activity of ICD that has been treated with AceK (but not further treated with potential small molecule regulators). **(B)** A similar experiment to that just described was also carried out with ICD_{EC} with $AceK_{EC}$. The *E. coli* AceK more profoundly inhibits *E. coli* ICD activity compared with the *P. aeruginosa* homologue AceK/ICD pair. All plots were generated using GraphPad Prism 6, and the errors bars correspond to ± 1 standard deviation. All experiments were performed in triplicate.

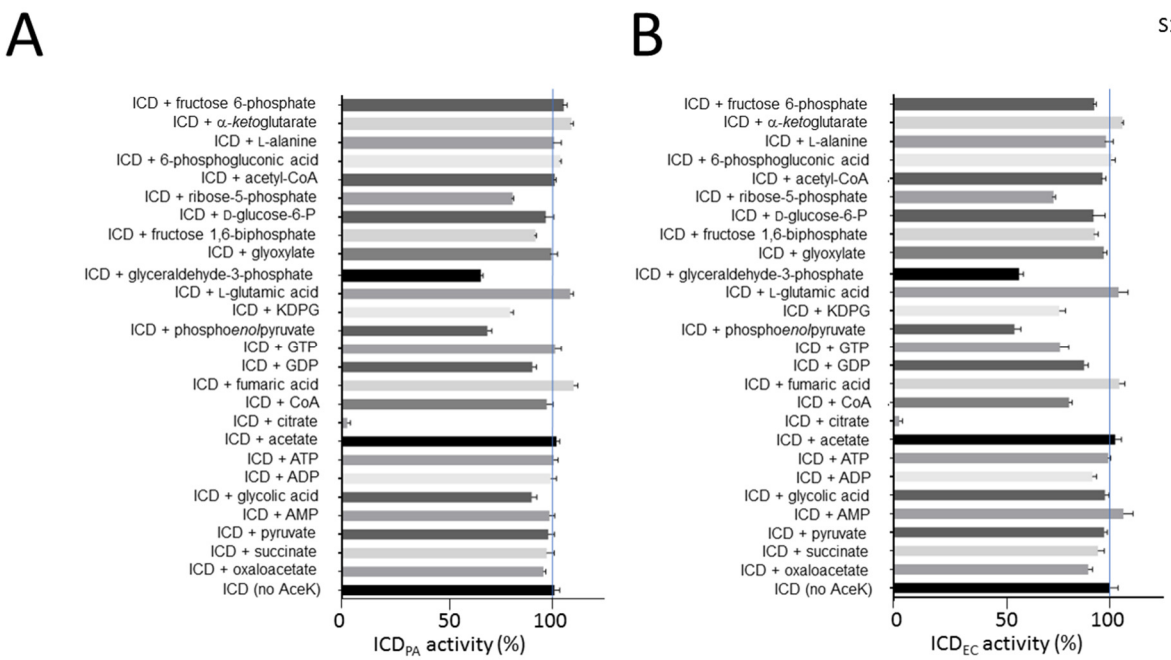

Figure S11. ICD *iso*citrate dehydrogenase activity is not intrinsically affected by most of the regulators that impact on AceK. **(A)** The metabolites tested as putative AceK regulators in **Figure S10** were also evaluated for their ability to directly activate/inhibit *P. aeruginosa* ICD. Note that ICD retains almost full activity in the presence of most of these compounds, although PEP, glyceraldehyde 3-phosphate, 2-*keto*-3-deoxyphosphogluconate, and ribose 5-phosphate slightly depress ICD activity when present at 5 mM, and citrate blocks ICD activity completely. **(B)** The same experiment as in (A) carried out with ICD_{EC}.

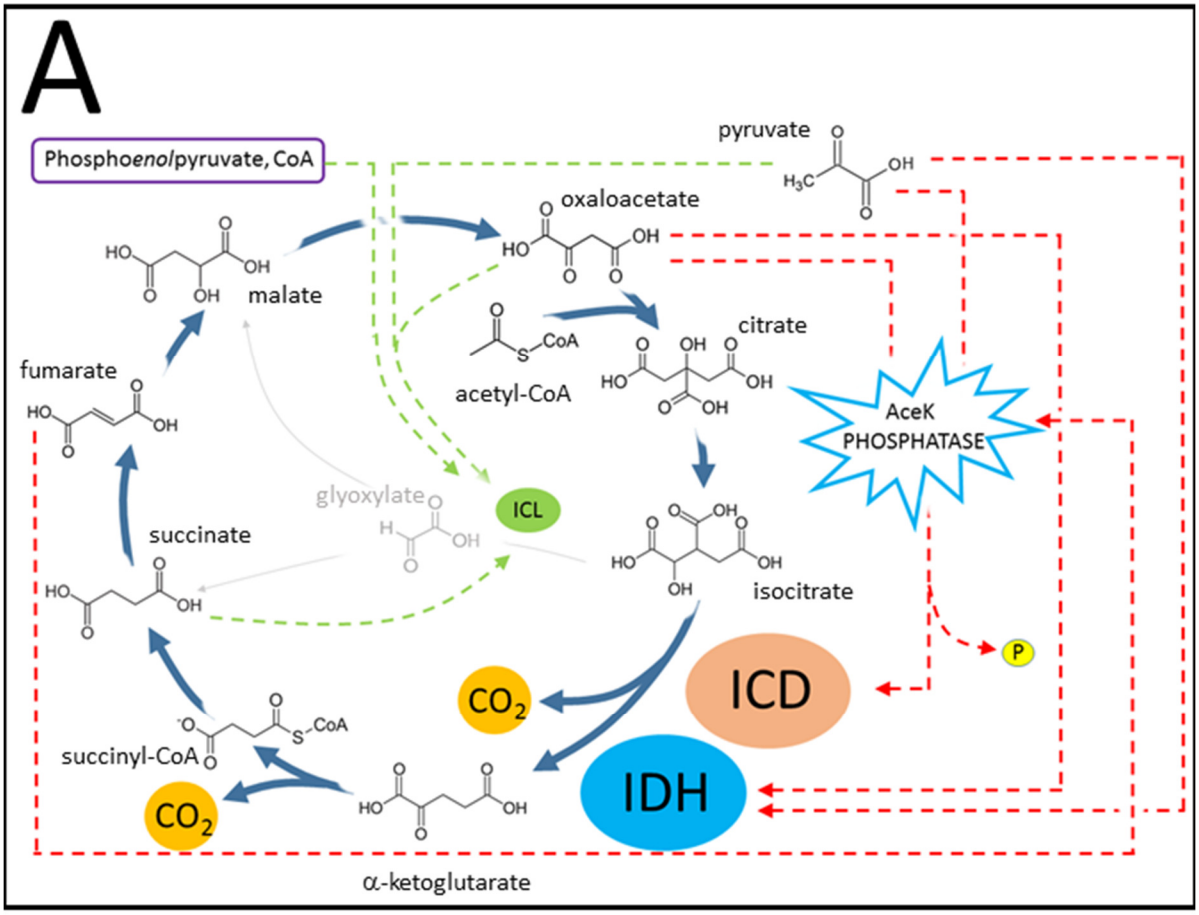
A
Phosphoenolpyruvate, CoA
pyruvate
oxaloacetate
malate
citrate
acetyl-CoA
fumarate
AceK
PHOSPHATASE
glyoxylate
ICL
succinate
isocitrate
P
ICD
CO2
succinyl-CoA
IDH
CO2
α-ketoglutarate

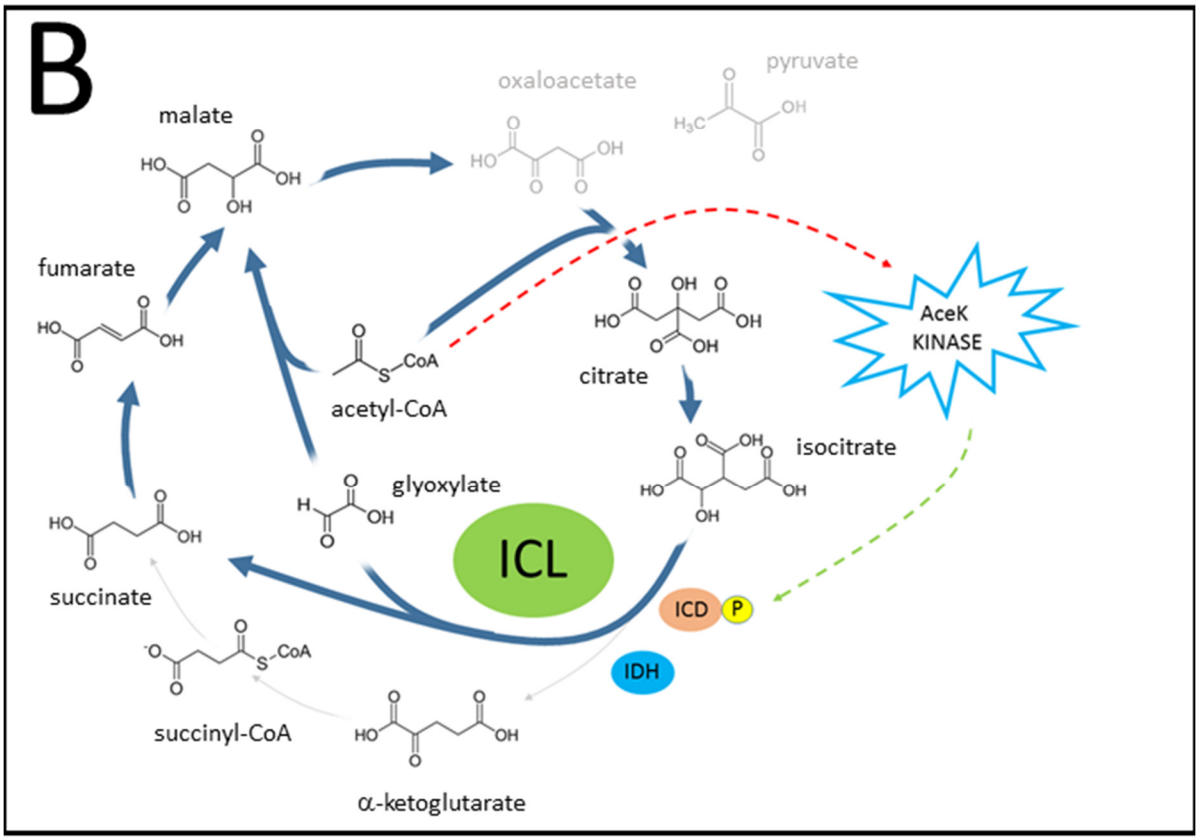
B
malate
oxaloacetate
pyruvate
fumarate
AceK
KINASE
acetyl-CoA
citrate
isocitrate
glyoxylate
ICL
succinate
ICD
P
IDH
succinyl-CoA
α-ketoglutarate

Figure S12. Regulation of flux partitioning between the glyoxylate shunt and the TCA cycle in *P. aeruginosa*. **(A)** Oxaloacetate and pyruvate are abundant. Along with phospho*enol*pyruvate, succinate and CoA, these compounds allosterically inhibit ICL. Pyruvate and oxaloacetate and also allosterically activate IDH. In parallel, the phosphatase activity of AceK is activated by pyruvate, oxaloacetate, fumarate, succinate and α-ketoglutarate, as well as the glycolytic intermediate, glyceraldehyde 3-phosphate, thereby disinhibiting ICD. Collectively, these changes favour flux through the TCA cycle and depress flux through the glyoxylate shunt. **(B)** When the gluconeogenic precursors, oxaloacetate and pyruvate are limiting (indicated by their grey shading), IDH activity is no longer stimulated and ICL becomes disinhibited, favouring flux through the glyoxylate shunt. Moreover, oxaloacetate limitation will give rise to an accumulation of its condensation partner, acetyl-CoA. This, in turn, activates the kinase activity of AceK, leading to the phosphorylation and consequent inhibition of ICD. *P. aeruginosa* also employs "rheostatic" control of IDH activity by glyoxylate and succinate. Here, as ICL activity increases beyond the capacity of downstream reactions to handle the products generated, the succinate inhibits ICL and the glyoxylate activates IDH. This auto-limits the flux through the glyoxylate shunt. Bold dark blue lines indicate enzymologically-favoured flux. Red dashed lines indicate stimulation. Green dashed lines indicate inhibition. The size of the ICL, IDH and ICD symbols indicates their relative activity.

	ICL	IDH	ICD
Data collection statistics			
Radiation source	Diamond (UK), I02	Diamond (UK), I04-1	Diamond (UK), I04-1
Wavelength (Å)	0.9795	0.9282	0.9282
Space group	I222	$C222_1$	$P12_11$
Cell dimensions			
a, b, c (Å)	80.94, 116.02, 128.53	126.46, 149.02, 201.13	88.88, 95.55, 104.01
α, β, γ (°)	90, 90, 90	90, 90, 90	90, 99, 90
Resolution range (Å)	1.88-29.49 (1.88-1.93)	2.71-29.62 (2.71-2.78)	2.70-47.78 (2.70-2.79)
Total reflections	614357 (27689)	940727 (66819)	304691 (17419)
Unique reflections	48986 (3287)	51799 (3682)	44233 (2978)
Multiplicity	12.5 (8.4)	18.2 (18.1)	6.9 (5.8)
Completeness (%)	99.4 (92.1)	99.6 (97.2)	98.0 (89.4)
Mean I/sigma(I)	21.7 (3.0)	17.3 (3.7)	17.9 (2.0)
R-merge	0.086 (0.656)	0.176 (0.891)	0.068 (0.826)
R-pim	0.036 (0.340)	0.059 (0.304)	0.028 (0.348)
CC-half	0.99 (0.78)	0.99 (0.92)	0.99 (0.79)
Refinement			
R_{work} (%)	18.32	20.80	24.56
R_{free} (%)	21.17	26.67	28.37
No. of molecules per ASU	1	2	4
No. of total atoms (no H)	3798	11551	12832
atoms for ligands	6	58	n/a
atoms for waters	182	197	36
Ramachandran plot analysis, number of residues in;			
Favoured regions (%)	96.90	93.91	92.19
Allowed regions (%)	2.69	5.54	7.03
Disallowed regions (%)	0.41	0.55	0.78
B-factor (Å^2)			
Average/Wilson	35.10/26.42	52.31/43.36	114.21/68.00
Ligands	52.86	28.88	n/a
Solvent	32.55	35.87	38.04
RMS deviations			
Bond lengths (Å)	0.01	0.01	0.003
Bond angles (°)	1.43	1.52	0.602
PDB entry	**6G1O**	**6G3U**	**5M2E**

Table S1. Crystallographic statistics